

Influence of neutron-pairs condensation on the charge radii difference of mirror nuclei*

Jing Huang (黄精)¹ Xiang Jiang (蒋翔)² Na Tang (唐娜)^{1,3} Rong An (安荣)^{1,4,3†}

¹School of Physics, Ningxia University, Yinchuan 750021, China

²College of Physics and Optoelectronic Engineering, Shenzhen University, Shenzhen 518060, China

³Key Laboratory of Beam Technology of Ministry of Education, School of Physics and Astronomy, Beijing Normal University, Beijing 100875, China

⁴Guangxi Key Laboratory of Nuclear Physics and Technology, Guangxi Normal University, Guilin, 541004, China

Abstract: Highly linear correlation between the charge radii difference of mirror-pair nuclei and the slope parameter of symmetry energy has been built in the existing literatures. In this work, the impact of neutron-proton correlation deduced from the neutron- and proton-pairs condensation around the Fermi surface on determining the slope parameter of nuclear symmetry energy is investigated based on the Skyrme density functionals. The differential charge radii of Ni isotopes are employed to inspect the validity of this recently developed model. The calculated results suggest that the modified model can reproduce the shell quenching of charge radii at the neutron number $N = 28$ along Ni isotopic chain. The shell closure effect of the charge radii can also be predicted at the neutron number $N = 50$. The correlations between the charge radii differences of mirror partner nuclei ^{32}Ar - ^{32}Si and ^{54}Ni - ^{54}Fe and the slope parameters of symmetry energy are also analyzed. It is shown that the covered range of the symmetry energy slope is influenced by the neutron-pairs condensation around the Fermi surface. Moreover, a relatively stiff equation of state can be inferred from the mirror pairs ^{32}Ar - ^{32}Si and ^{54}Ni - ^{54}Fe when the influence coming from the neutron-pairs condensation is taken into account.

Keywords: charge radii, shell closure effect, mirror nuclei, slope parameter of symmetry energy, equation of state

DOI: CSTR:

I. INTRODUCTION

As accurately measured quantities in terrestrial laboratories, charge radii are generally used to encode the nuclear structure phenomena, such as the shape-phase transition [1–6], shell quenching phenomena [7–13], and the odd-even staggering (OES) effects [14–19]. Precise knowledge of nuclear size plays an indispensable role in the course of nuclear physics and astrophysics [20]. Especially, charge radii difference in mirror-paired nuclei naturally defined with neutron number N and proton number Z exchanged but with the same mass number $A = N + Z$ is intimately associated with our understanding of the fundamental interactions. The highly linear correlation between the difference of charge radii of mirror partner nuclei (ΔR_{ch}) and the symmetry energy slope (L) was

firstly proposed in Ref. [21]. Then more researches have verified that the charge radii differences of mirror-pair nuclei are linearly correlated with the slope parameter of symmetry energy [22–31].

Owing to the advanced techniques in experiments, much more data on charge radii of nuclei far away from the β -stability line have been accumulated [32, 33]. Generally, nucleus can be regarded as the incompressible liquid-drop, and its size can be ruled by the $A^{1/3}$ or $Z^{1/3}$ law [34–36]. However, the microscopic aspects cannot be featured yet, such as the information about proton density distributions and single particle levels. The relativistic mean field theory [37, 38] and non-relativistic Skyrme Hartree-Fock-Bogoliubov (HFB) approach [39, 40] can also be used to describe the systematical evolution of nuclear charge radii as well, but the local variations of

Received 11 February 2025; Accepted 7 May 2025

* This work was supported by the Open Project of Guangxi Key Laboratory of Nuclear Physics and Nuclear Technology, No. NLK2023-05, the Central Government Guidance Funds for Local Scientific and Technological Development, China (No. Guike ZY22096024), the Natural Science Foundation of Ningxia Province, China (No. 2024AAC03015), and the Key Laboratory of Beam Technology of Ministry of Education, China (No. BEAM2024G04). X. J. was grateful for the support of the National Natural Science Foundation of China under Grants No. 11705118, No. 12175151, and the Major Project of the GuangDong Basic and Applied Basic Research Foundation (2021B0301030006). N. T. was grateful for the support of the key research and development project of Ningxia (Grants No. 2024BEH04090) and the Key Laboratory of Beam Technology of Ministry of Education, China (No. BEAM2024G05)

† E-mail: rongan@nxu.edu.cn

©2025 Chinese Physical Society and the Institute of High Energy Physics of the Chinese Academy of Sciences and the Institute of Modern Physics of the Chinese Academy of Sciences and IOP Publishing Ltd. All rights, including for text and data mining, AI training, and similar technologies, are reserved.

nuclear charge radii cannot be captured adequately along a long isotopic chain.

Fine structures of nuclear charge radii can be influenced by various underlying mechanisms [41]. With considering the density gradient terms in its pairing interactions part, the discontinuous behavior of charge radii can be described well [42]. Shown in Refs. [27, 43], the correlations between the charge radii differences of mirror-pair nuclei and the slope parameter of symmetry energy are reduced by the pairing effects. Meanwhile, the shape deformation can also have an influence on determining the local variations of nuclear charge radii [1, 6]. As mentioned in Ref. [30], the quadrupole deformation correction has been taken into account in describing the charge radii difference of ^{32}Ar - ^{32}Si , but the influence coming from shape deformation can almost be negligible. Besides, recent studies suggest that the compression modulus of finite nuclei cannot be ignored in ascertaining the slope parameter of symmetry energy [43, 44].

The short-range correlations between neutrons and protons have an influence on determining the charge density distributions around the Fermi surface [45–47]. This means that neutron-proton correlations should be considered appropriately in describing the bulk properties of finite nuclei [48, 49]. Meanwhile, a strong coupling between neutron- and proton-pairing correlations (being α -clusters) [50] or a residual effective four-body force [51] plays an indispensable role in describing the local variations of the nuclear charge radii. Based on the relativistic mean-field model, a novel ansatz derived from the neutron- and proton-pairs condensation around the Fermi surface has been incorporated into the root-mean-square (rms) charge radii formula [52]. This recently developed approach can reproduce the systematic evolution of nuclear charge radii including those the corresponding OES phenomena and shell closure effects [53–56]. Furthermore, this suggests that the correlation between the neutron- and proton-pairs condensation around the Fermi surface actually plays an indispensable role in describing the systematic trend of changes of nuclear charge radii.

As demonstrated above, the proton density distributions in mirror nuclei can provide an alternative access to ascertain the equation of state of isospin asymmetric nuclear matter. It is also worth noting that the influence of neutron-pairs condensation on determining the charge radii differences of mirror-paired nuclei are hardly found in the existing literatures. Therefore, the influences of neutron-pairs condensation on the determination of the charge radii differences should also be investigated based on the Skyrme EDFs. In our calculations, the spherical Hartree-Fock-Bogoliubov (HFB) framework is employed and the differential mean-square charge radii of Ni isotopes are further used to test the validity of this developed model. Moreover, the charge radii differences of mirror-pair nuclei ^{32}Ar - ^{32}Si and ^{54}Ni - ^{54}Fe are also applied

to analyze the correlation between the charge radii difference of mirror partner nuclei and the nuclear symmetry energy slope.

The outline of the present paper is the following. In Section II, the theoretical framework is very briefly presented. In Section III, the numerical results and discussion are provided. Finally, a summary together with some perspectives are given in Section IV.

II. THEORETICAL FRAMEWORK

The Skyrme density functional has made considerable success in describing various physical phenomena [39, 40, 57–59]. In our calculations, the Skyrme-like effective interaction has been recalled as follows [60, 61],

$$\begin{aligned} V(\mathbf{r}_1, \mathbf{r}_2) = & t_0(1 + x_0 \mathbf{P}_\sigma) \delta(\mathbf{r}) \\ & + \frac{1}{2} t_1(1 + x_1 \mathbf{P}_\sigma) [\mathbf{P}'^2 \delta(\mathbf{r}) + \delta(\mathbf{r}) \mathbf{P}'^2] \\ & + t_2(1 + x_2 \mathbf{P}_\sigma) \mathbf{P}' \cdot \delta(\mathbf{r}) \mathbf{P} \\ & + \frac{1}{6} t_3(1 + x_3 \mathbf{P}_\sigma) [\rho(\mathbf{R})]^\alpha \delta(\mathbf{r}) \\ & + iW_0 \sigma \cdot [\mathbf{P}' \times \delta(\mathbf{r}) \mathbf{P}] . \end{aligned} \quad (1)$$

Here, $\mathbf{r} = \mathbf{r}_1 - \mathbf{r}_2$ and $\mathbf{R} = (\mathbf{r}_1 + \mathbf{r}_2)/2$ are naturally related to the positions of two nucleons \mathbf{r}_1 and \mathbf{r}_2 , $\mathbf{P} = (\nabla_1 - \nabla_2)/2i$ represents the relative momentum operator acting on the right and the corresponding counterpart $\mathbf{P}' = -(\nabla'_1 - \nabla'_2)/2i$ characterizes its complex conjugate acting on the left, and $\mathbf{P}_\sigma = (1 + \vec{\sigma}_1 \cdot \vec{\sigma}_2)/2$ represents the spin exchange operator that be used to dominate the relative strength of the $S = 0$ and $S = 1$ channels for a given term in the two-body interactions, with $\vec{\sigma}_{1(2)}$ being the Pauli matrices. The last term features the spin-orbit force, in which $\sigma = \vec{\sigma}_1 + \vec{\sigma}_2$. The quantities α , t_i , x_i ($i = 0-3$), and W_0 represent the parameters of the effective forces used in this work.

The pairing correlations can be generally treated either by the BCS method or by the Bogoliubov transformation [37, 39, 40, 62–64]. In this work, the Bogoliubov transformation is used to treat the pairing correlations. The density-dependent zero-range pairing force is employed as follows [65, 66],

$$V_{\text{pair}}(\mathbf{r}_1, \mathbf{r}_2) = V_0 \left[1 - \eta \left(\frac{\rho(\mathbf{r})}{\rho_0} \right) \right] \delta(\mathbf{r}_1 - \mathbf{r}_2). \quad (2)$$

Here, $\rho(\mathbf{r})$ is the baryon density distribution in coordinate space and $\rho_0 = 0.16 \text{ fm}^{-3}$ represents the nuclear saturation density. Generally, the values of η are taken as 0.0, 0.5, or 1.0 for volume-, mixed-, or surface-type pairing interactions, respectively. As mentioned in Refs. [27, 43], the pairing correlations have an influence on determining the

correlation between the charge radii difference of mirror-pair nuclei and the slope parameter of symmetry energy. Therefore, the mixed-type pairing force is chosen in our calculations. The quantity V_0 is adjusted by calibrating the empirical energy gaps with three-point formula [65, 67]. The single-particle energy levels and wave functions of the constituent nucleons can be obtained by solving the HFB equations with the self-consistent iteration method [68].

The range of the proton matter distributions can be deduced from the wave functions of the constituent protons. The quantity of nuclear charge radius (R_{ch}) can be defined as the root-mean-square radius of its proton distribution, which can be calculated through the following expression (in units of fm²) [55],

$$R_{\text{ch}}^2 = \langle r_p^2 \rangle + 0.7056 + \frac{a_0}{\sqrt{A}} \Delta \mathcal{D} + \frac{\delta}{\sqrt{A}}. \quad (3)$$

The first term $\langle r_p^2 \rangle$ represents the charge density distributions of point-like protons and the second one is attributed to the finite size of protons [69]. For the third term, the expression $\Delta \mathcal{D}$ is defined as $\Delta \mathcal{D} = |\mathcal{D}_n - \mathcal{D}_p|$. The quantity of \mathcal{D}_n (\mathcal{D}_p) is recalled as follows,

$$\mathcal{D}_{n,p} = \sum_{k>0}^{n,p} u_k v_k, \quad (4)$$

where $v_k^{n,p}$ is the amplitude of the occupation probability of the k th quasi-particle orbital for neutron or proton at the canonical basis, and $u_k^2 = 1 - v_k^2$. It is also mentioned that the quantity of $\mathcal{D}_{n,p}$ can be used to measure the Cooper pairs condensation around the Fermi surface [70, 71]. The expression of $\Delta \mathcal{D}$ is used to measure the neutron- and proton-pairs correlation around the Fermi surface [17, 52]. The parameter set $a_0 = 0.561$ is adjusted by reproducing the parabolic-like shape and odd-even oscillation behaviors in the charge radii of K and Ca isotopes [55]. The last term is considering the correlation between the simultaneously unpaired neutron and proton. For mirror pair nuclei, the difference in charge radii (ΔR_{ch}) can be obtained through the formula Eq. (3). Actually, the last term is invalid due to the time-reversal symmetry is assumed in this work, namely restricting ourselves to even-even nuclei.

III. RESULTS AND DISCUSSION

The influence of neutron-proton correlation deduced from the neutron- and proton-pairs condensation around the Fermi surface has been incorporated into the rms charge radii formula based on the relativistic EDFs [52–56]. However, the corresponding discussion is hardly found in the Skyrme EDFs. Firstly, the differential mean-

square charge radii of Ni isotopes are employed to review the validity of this theoretical model based on the Skyrme density functional model. The mixed-type pairing interaction is used and the pairing strength is chosen to $V_0 = 370.2$ MeV fm³ by adjusting the empirical energy gap along the Ni isotopes. This is in accord with Ref. [43]. Two pairs of mirror nuclei ³²Ar-³²Si and ⁵⁴Ni-⁵⁴Fe are used to inspect the influence of neutron-proton correlations on determining the charge radii difference of the corresponding mirror-pair nuclei. For the convenience of our discussion, the results obtained by Eq. (3) are labeled by HFB*. While the results obtained by the approach without considering the influence coming from the neutron- and proton-pairs condensation are marked by HFB.

Shell closure effects of charge radii are generally observed throughout the whole nuclear chart [32, 33]. As mentioned in Ref. [72], Skyrme EDFs cannot describe the shell closure effect in nuclear charge radii well. Recently developed RMF(BCS)* model can characterize the discontinuous behaviors of nuclear charge radii, especially the shell quenching phenomena [55]. Therefore, it is worthwhile to use this method to ascertain the slope parameter of symmetry energy. The parameter sets of the effective forces used in this work and the corresponding values of the bulk properties of symmetric nuclear matter are shown explicitly in Table 1. Under the specific incompressibility coefficients K , the slope parameter L and symmetry energy E_{sys} at saturation density ρ_0 cover long range. It should be mentioned that the correlation between the charge radii differences of mirror partner nuclei and the slope parameter of symmetry energy can be influenced by the incompressibility coefficients of symmetry nuclear matter [43, 44]. Meanwhile, giant monopole resonances provide the value of the isoscalar incompressibility $K = 230 \pm 10$ MeV [73, 74]. Thus the parameter sets s3032 and s4032 classified by the almost similar slope parameters but different incompressibility coefficients are chosen in describing the differential charge radii of Ni isotopes.

Charge radii of Ni isotopes have been detected accurately through collinear laser spectroscopy approach [24, 72, 75]. The extracted results suggest that the shell quenching phenomenon in charge radii can be observed significantly around the fully filled $N = 28$ shell. Moreover, across the neutron number $N = 28$, the trend of changes in the charge radii is similar to the Ca isotopic chain. Actually, the systematic evolution of nuclear charge radii across the $N = 28$ shows the similar trend from K to Zn isotopic chains, namely that is almost independent of the atomic number [55, 76].

As shown in Fig. 1, the differential charge radii of Ni isotopes with respect to reference nucleus ⁵⁶Ni are depicted by the HFB and HFB* methods with the effective forces s3032 and s4032, respectively. It can be seen that HFB* model can reproduce the trend of changes of charge

Table 1. Saturation properties of the Skyrme parametrization sets used in this work [43], such as the incompressibility coefficients K (MeV), slope parameter L (MeV) and symmetry energy E_{sys} (MeV) at saturation density ρ_0 (fm^{-3}), are shown.

K (MeV)	Sets	L (MeV)	E_{sys} (MeV)
$K \approx 230$ MeV	s3028	-11.2262	28
	s3030	22.8715	30
	s3032	36.2246	32
	s3034	56.1442	34
	s3036	71.5428	36
	s3038	87.6155	38
	s3040	106.0862	40
	s4028	3.9774	28
$K \approx 240$ MeV	s4030	34.0735	30
	s4032	34.4283	32
	s4034	62.5884	34
	s4036	75.6679	36
	s4038	98.6522	38
	s4040	108.1741	40
	s5028	33.0037	28
	s5030	30.0248	30
$K \approx 250$ MeV	s5032	43.5871	32
	s5034	60.3202	34
	s5036	80.1762	36
	s5038	97.4925	38
	s5040	112.2079	40

radii across the $N = 28$ shell closure along Ni isotopic chain as shown in Fig. 1 (a). Meanwhile, the decreased trend of charge radii from ^{54}Ni to ^{56}Ni can be reproduced as well. This leads to the significantly observed kink phenomenon at the neutron number $N = 28$. Here, it can be found that the values of charge radii for isotopes $^{60,62}\text{Ni}$ are slightly underestimated for the s3032 effective force. In contrast to HFB* model, the differential charge radii of Ni isotopes cannot be reproduced by the HFB model. Particularly, the rapid increase of charge radii cannot be reproduced well across the fully filled $N = 28$ shell. The same scenario can also be encountered around $N = 50$ where the HFB model cannot represent the shrinking trend of charge radii. By contrast, shell quenching phenomenon in charge radii of Ni isotopes could be predicted at the neutron number $N = 50$ through the HFB* model.

As is well known, the inverted parabolic-like shape of charge radii can be evidently observed between the neutron numbers $N = 20$ and $N = 28$ along K and Ca isotopes [32, 33]. The inverted parabolic-like shape of charge radii

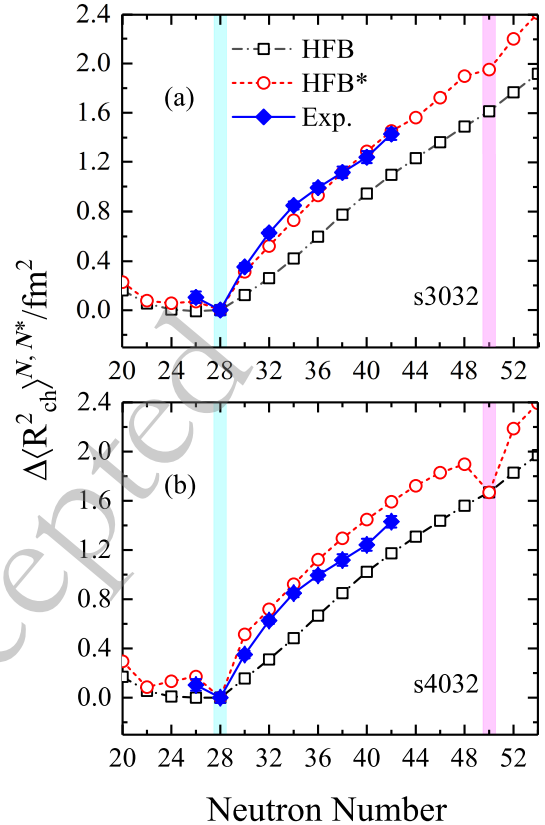


Fig. 1. (Color online) Mean-square charge radii differences of the even-even Ni isotopes relative to the ^{56}Ni nucleus obtained by the Skyrme EDFs with the parameter sets s3032 (a) and s4032 (b) are presented for HFB (open square) and HFB* (open circle) methods. The experimental data are taken from the Refs. [24, 32, 33, 72, 75] (solid diamond). The shadowed planes mark the neutron magic numbers $N = 28$ (light blue) and $N = 50$ (light pink), respectively.

along Ni isotopic chain can be obtained by the HFB* model between the neutron numbers $N = 20$ and $N = 28$. However, this phenomenon cannot be represented in the HFB model. This can be found obviously that the trend of change of charge radius for ^{54}Ni isotope cannot be reproduced well by the HFB model. Moreover, the inverted parabolic-like shape of charge radii obtained by the HFB* model can also be found between the neutron numbers $N = 28$ and $N = 50$. Thus more experimental data are urgently required in future research.

In Fig. 1 (b), the results obtained by the HFB and HFB* models are drawn with the effective force s4032. The shell quenching effects of charge radii at the neutron numbers $N = 28$ and $N = 50$ can also be emerged from the HFB* model. However, the differential charge radii of $^{66,68,70}\text{Ni}$ isotopes obtained by the HFB* model are slightly deviated from the experimental data. Here, it should be mentioned that the HFB model still underestimates the systematic trend of changes of charge radii in the Ni isotopes. Significant deviations can be found between the

absolute values obtained by the effective force s3032 and experimental ones with respect to those calculated by the effective force s4032. The stability properties of finite nuclei are mostly determined by the Coulomb force and the symmetry energy. The larger symmetry energy means that more strong isospin interactions can be captured, which leads to the larger range of the charge density distributions radii [77]. In our calculations, the remarkably shrunken phenomenon of the differential charge radii at the neutron number $N = 50$ can be obtained by the parameter set s4032 compared to the effective force s3032. This is due to the fact that the symmetry energy slope is almost similar but with different incompressibility coefficients. This can be understood easily from the charge radius of ^{78}Ni , in which the value of charge radius for ^{78}Ni obtained through the s3032 force is larger than the case calculated with effective force s4032 about 0.02 fm. It suggests that the effective force s4032 gives more compact properties in finite nuclei.

Accurate description of nuclear charge radii provides a sensitive indicator to our understanding of fundamental interactions in exotic nuclei. As mentioned in Refs. [46, 49, 78], isospin interactions coming from the neutron-proton correlations should be considered properly in evaluating the nuclear size. A greater ability of the HFB* model to reproduce the differential charge radii of Ni isotopes is attributed to the neutron-proton correlations deduced from the neutron-pairs and proton-pairs condensation around the Fermi surface. This is actually in accord with those in Refs. [79–81] where the neutron-proton interactions derived from the valence neutrons and protons can describe the local variations of nuclear charge radii along a long isotopic chain. This further suggests that the neutron-proton correlations around the Fermi surface play an indispensable role in determining the discontinuous variations of nuclear charge radii.

Highly linear correlation between the charge radii difference (ΔR_{ch}) of mirror-pair nuclei and the slope parameter (L) of symmetry energy has been utilized to ascertain the isospin components in the equation of state of asymmetric nuclear matter [21–31]. Therefore, it is theoretically essential to further review the influence of neutron-proton correlations on determining the values of ΔR_{ch} in a given pair of mirror nuclei. In our calculations, mirror nuclei with mass number $A = 32$ and 54 are employed to illustrate the influence of neutron-proton correlations on the charge radii difference. The corresponding experimental data are shown in Table 2.

The theoretical results obtained by HFB and HFB* models are used to access the correlation between ΔR_{ch} and L . As shown in Fig. 2, the results of ΔR_{ch} for mirror partner nuclei ^{54}Ni - ^{54}Fe and ^{32}Ar - ^{32}Si are shown as a function of slope parameter L . The shadowed planes indicate the systematic uncertainties of the charge radii difference between the corresponding mirror nuclei, which cover the

Table 2. Charge radii (R_{ch}) and charge radii difference (ΔR_{ch}) databases for the $A = 32$ and 54 mirror pairs nuclei. The parentheses on the values of charge radii and the differences of charge radii are shown with systematic uncertainties [24, 30, 32, 33].

A		R_{ch} (fm)	ΔR_{ch} (fm)
32	Ar	3.3468(62)	
	Si	3.153(12)	0.194(14)
54	Ni	3.7370(30)	
	Fe	3.6880(17)	0.049(4)

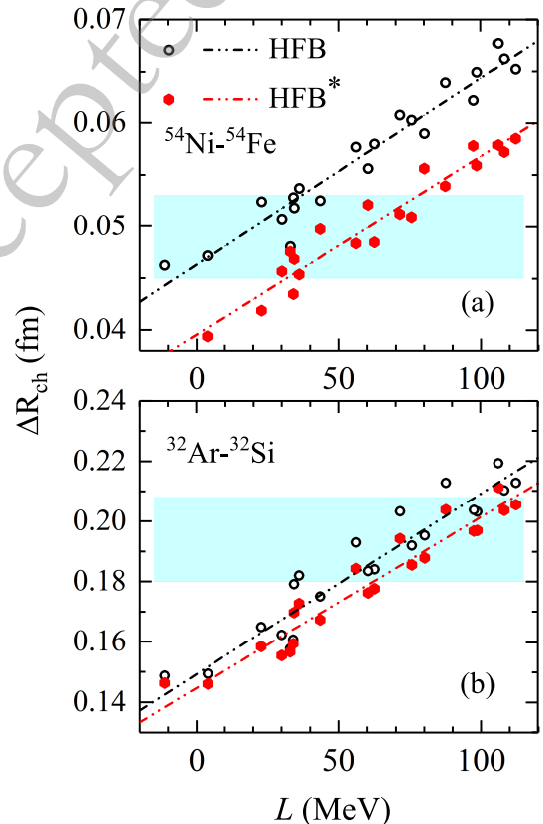


Fig. 2. (Color online) ΔR_{ch} of mirror partner nuclei ^{54}Ni - ^{54}Fe (a) and ^{32}Ar - ^{32}Si (b) obtained by the HFB (open circle) and HFB* (solid pentagon) methods as a function of slope parameter L at saturation density ρ_0 . The experimental results are shown as horizontal light blue bands. The dot-dot-dashed lines indicate the corresponding theoretical linear fits.

ranges of 0.049(4) fm (^{54}Ni - ^{54}Fe) and 0.194(14) fm (^{32}Ar - ^{32}Si), respectively. The results obtained using the HFB and HFB* models display the approximately linear correlation between ΔR_{ch} and L for both pairs of mirror nuclei. Generally, the uncertainty range of ΔR_{ch} covered by the fitted line is used to constrain the slope parameter L . It should be mentioned that the covered range of L is changed obviously by the HFB* model.

Here, the lower limit of L is constrained at 0.0 MeV

in our discussion. As shown in Fig. 2 (a), the coved range of L obtained by the HFB model falls into $0.0 \leq L \leq 38.11 (\pm 5.07)$ MeV. By contrast, HFB^* model gives the range of $33.18 \leq L \leq 78.64 (\pm 3.58)$ MeV. This is in accord with Ref. [24] where the deduced L value falls into the range $21 \leq L \leq 88$ MeV. This means that the neutron-proton correlations around the Fermi surface can influence the determination of the values of ΔR_{ch} . Moreover, the larger deviation can also be encountered in the mirror pair nuclei ^{32}Ar - ^{32}Si . The range of $51.22 \leq L \leq 97.87 (\pm 6.17)$ MeV can be extracted from ^{32}Ar - ^{32}Si with the HFB method. The HFB^* method gives the range of $62.21 \leq L \leq 111.59 (\pm 5.19)$ MeV. As demonstrated in Ref. [30], the rather soft equation of state (EoS) has been obtained, namely $L \leq 60$ MeV. However, a stiffer EoS can be extracted from the charge radii difference of mirror pair nuclei ^{32}Ar - ^{32}Si in our calculations. Our results suggest that HFB^* model seems to give rather stiff EoS than those obtained by the HFB model. Furthermore, it seems to suggest that the neutron-proton correlations should be considered properly in constraining the slope parameter L . As mentioned in Refs. [43, 44, 82], the quantification uncertainty suffering from nuclear matter incompressibility is inevitable in evaluating the isospin components. As shown in Fig. 2, the influence coming from the nuclear matter incompressibility coefficients cannot be distinguished clearly in discussing the correlation between the charge radii differences of mirror partner nuclei and the slope parameter of symmetry energy. This may lead to the relatively larger uncertainty ranges in evaluating the slope parameter L .

To facilitate the quantitative comparison under various incompressibility coefficients, the ΔR_{ch} of ^{54}Ni - ^{54}Fe obtained by the HFB and HFB^* models is depicted as a function of the slope parameter L shown in Fig. 3. The effective forces classified by various incompressibility coefficients K are used to distinguish the covered range of the slope parameters of symmetry energy. Here it should be mentioned that the covered ranges of the slope parameter L obtained by the HFB method are distinguished evidently from the results obtained by the HFB^* model in the mirror-pair nuclei ^{54}Ni - ^{54}Fe . For the specific incompressibility coefficients, the covered lower and upper ranges of L are simultaneously enlarged with considering the neutron-proton correlations around the Fermi surface. However, for $K = 230$ MeV and $K = 240$ MeV, the covered ranges of L are almost similar for HFB^* model. In contrast to $K = 230$ MeV and $K = 240$ MeV, HFB^* model gives the relatively lower range of L when the effective forces classified by $K = 250$ MeV are used.

As mentioned above, the incompressibility coefficient has an influence on the determination of the symmetry energy slope. As shown in Fig. 4, ΔR_{ch} of ^{32}Ar - ^{32}Si as a function of L is also shown with the HFB and HFB^* models. For the parameter set classified by various in-

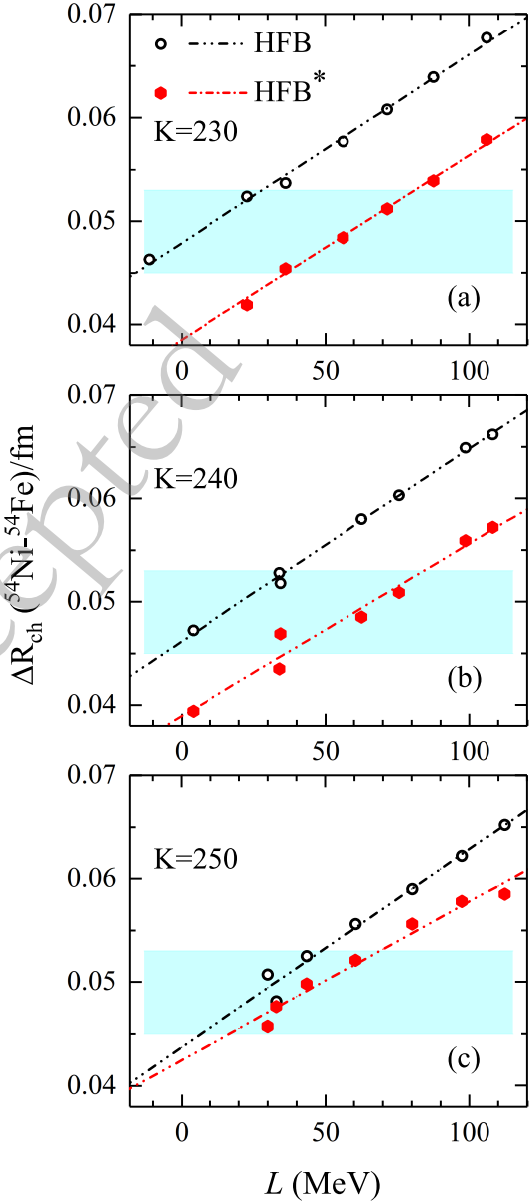


Fig. 3. (Color online) ΔR_{ch} of mirror-pair nuclei ^{54}Ni - ^{54}Fe as a function of slope parameter L at the saturation density ρ_0 . The open circle represents the HFB calculations and the solid pentagon represents the results obtained by HFB^* model. The experimental data are depicted as the light blue shadowed band. The dot-dot-dashed line indicates theoretical linear fits.

compressibility coefficients, the upper and lower limit ranges of the slope parameter L obtained by the HFB^* model are systematically enlarged with respect to those obtained by the HFB method. For $K = 240$ MeV and $K = 250$ MeV, the covered ranges of L are almost similar for HFB^* model. However, for $K = 230$ MeV case, the upper range of L is more lower than the $K = 240$ MeV and $K = 250$ MeV cases, namely about 20 MeV. This further suggests that the correlation between the charge radii difference of mirror partner nuclei and the slope parameter

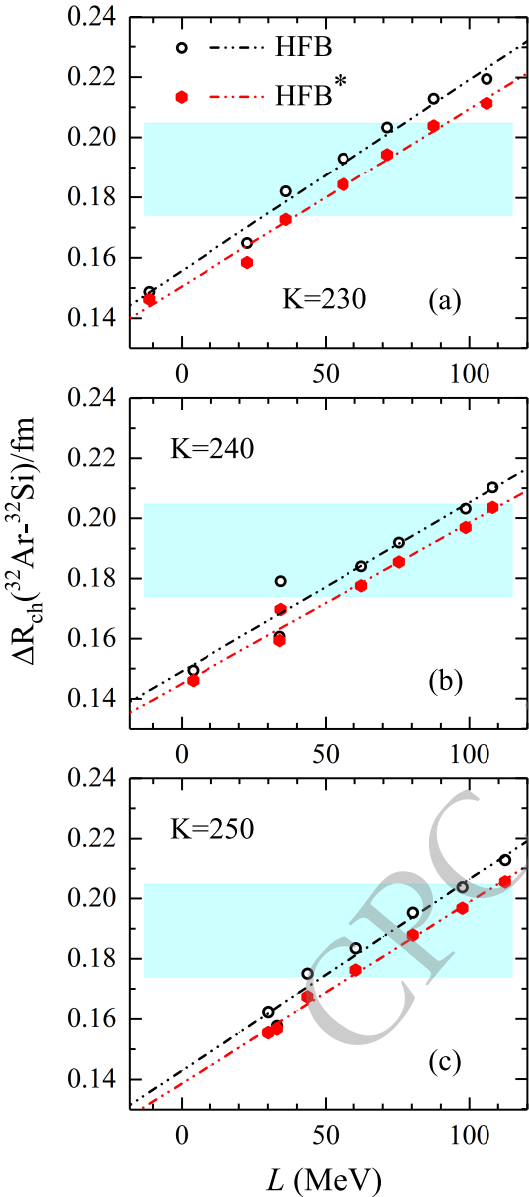


Fig. 4. (Color online) Same as Fig. 3 but for mirror-pair nuclei ^{32}Ar - ^{32}Si .

er of symmetry energy can be influenced by the effective forces classified by various incompressibility coefficients. In Table 3, the charge radii of mirror partner nuclei ^{32}Ar - ^{32}Si and ^{54}Ni - ^{54}Fe are shown with various effective forces classified by the incompressibility coefficients $K \approx 230, 240$, and 250 MeV.

Generally, neutron skin thickness of a heavy nucleus provides a superior access to constrain the equation of state of isospin asymmetric nuclear matter. The difference of proton density distributions in mirror nuclei is intimately related to the neutron skin thickness [25, 83]. This indicates that the information about neutron skin thickness can be extracted from the directly measured charge radii data. As demonstrated in Refs. [84, 85], the

precise data on mirror charge radii cannot make a rigorous constraint on the slope parameter L , even the worse correlation can be obtained between the mirror charge radii difference ΔR_{ch} and the slope parameter L . The bulk properties of finite nuclei cannot be captured adequately by the effective forces deduced from the infinite nuclear matter. This can be understood from some specific aspects those characterize the radii range of the proton density distributions, such as shell closure effect [11, 86] and the influence coming from isospin symmetry breaking [87-89]. Actually, the proton and neutron matter distributions are mutually influenced by each other. As discussed in this paper, the neutron-proton correlations deduced from the neutron-pairs and proton-pairs condensation around the Fermi surface and the compression modulus have an influence on determining the charge radii difference of mirror nuclei. Therefore, the influence derived from the neutron-proton correlations around the Fermi surface and the compression modulus of symmetry nuclear matter cannot be negligible in describing the nuclear charge radii [43, 55].

IV. SUMMARY

In this work, the influence of the neutron-pairs condensation around the Fermi surface on the determination of symmetry energy slope is investigated for the first time based on the Skyrme EDFs. The validity of this theoretical model has been reviewed by reproducing the trend of changes of differential charge radii along Ni isotopes. The differential charge radii of Ni isotopes can be described well by this modified model. Especially, the kink phenomenon in charge radii can be significantly reproduced at the neutron number $N = 28$ through this modified model. Meanwhile, the shell closure effect at $N = 50$ can also be expected in the charge radii of Ni isotopes. Intriguingly, the inverted parabolic-like shape in charge radii can be predicted between the neutron numbers $N = 20$ and $N = 28$ as well. The same scenario can also be observed between the $N = 28$ and $N = 50$, but the amplitude is apparently weakened.

As is well known, nuclear symmetry energy plays an essential role in various simulated codes [90-102]. Therefore, available density dependence of symmetry energy is required from multimessenger constraints. The correlations between the differences of charge radii of mirror partner nuclei ^{32}Ar - ^{32}Si and ^{54}Ni - ^{54}Fe and the slope parameters of symmetry energy can be affected by the neutron-proton correlations around the Fermi surface and the effective forces classified by various isoscalar incompressibility coefficients. Especially, the rather stiff equation of state can be obtained by the HFB* model in comparison to those deduced from the HFB method. The mean-square charge radius of a nucleus is naturally extracted from the charge density distributions. Recent

Table 3. Charge radii of mirror-pair nuclei ^{32}Ar - ^{32}Si and ^{54}Ni - ^{54}Fe (in units of fm) are shown with various effective forces classified by the incompressibility coefficients $K \approx 230$, 240, and 250 MeV.

	Sets	HFB			HFB*			
		^{32}Si	^{32}Ar	^{54}Fe	^{54}Ni	^{32}Si	^{32}Ar	^{54}Fe
$K \approx 230 \text{ MeV}$	s3028	3.1984	3.3471	3.7752	3.8215	3.2366	3.3829	3.7856
	s3030	3.2275	3.3923	3.7893	3.8417	3.2346	3.3930	3.8002
	s3032	3.2086	3.3906	3.7807	3.8344	3.2327	3.4054	3.7902
	s3034	3.2101	3.4031	3.7847	3.8424	3.2331	3.4174	3.7945
	s3036	3.2047	3.4080	3.7830	3.8438	3.2305	3.4248	3.7929
	s3038	3.2027	3.4155	3.7844	3.8483	3.2298	3.4337	3.7944
	s3040	3.2070	3.4263	3.7892	3.8569	3.2289	3.4402	3.7998
	s4028	3.2173	3.3667	3.7628	3.8100	3.2222	3.3682	3.7716
$K \approx 240 \text{ MeV}$	s4030	3.2590	3.4196	3.7828	3.8356	3.2638	3.4231	3.7921
	s4032	3.1821	3.3612	3.7325	3.7843	3.2066	3.3763	3.7869
	s4034	3.1996	3.3836	3.7528	3.8108	3.2078	3.3854	3.7624
	s4036	3.1938	3.3857	3.7488	3.8091	3.2029	3.3884	3.7585
	s4038	3.2043	3.4075	3.7641	3.8290	3.2131	3.4101	3.7741
	s4040	3.1898	3.4001	3.7504	3.8166	3.2012	3.4049	3.7605
	s5028	3.1991	3.3578	3.7298	3.7774	3.2327	3.3893	3.7564
	s5030	3.2018	3.3640	3.7388	3.7895	3.2110	3.3664	3.7457
$K \approx 250 \text{ MeV}$	s5032	3.1988	3.3738	3.7377	3.7902	3.2138	3.3811	3.7435
	s5034	3.1984	3.3819	3.7402	3.7958	3.2127	3.3889	3.7463
	s5036	3.2039	3.3992	3.7495	3.8085	3.2198	3.4076	3.7554
	s5038	3.2040	3.4078	3.7524	3.8146	3.2194	3.4162	3.7587
	s5040	3.1971	3.4099	3.7218	3.7870	3.2143	3.4198	3.7478
	s5042	3.1988	3.4111	3.7241	3.7902	3.2155	3.4211	3.7504
	s5044	3.1984	3.4123	3.7253	3.7914	3.2158	3.4223	3.7516
	s5046	3.1988	3.4135	3.7265	3.7926	3.2161	3.4235	3.7528

study suggests that charge radii can be derived from the charge-changing cross section measurements of exotic nuclei [103, 104]. Moreover, the difference of charge-changing cross section of mirror nuclei can also provide an alternative approach to evaluate the equation of state

of nuclear matter [105]. Thus a unified model is required in ascertaining the slope parameter of symmetry energy through the charge radii difference of mirror-paired nuclei.

References

- [1] T. Togashi, Y. Tsunoda, T. Otsuka, *Phys. Rev. Lett.* **117**, 172502 (2016)
- [2] A. E. Barzakh, D. V. Fedorov, V. S. Ivanov, *Phys. Rev. C* **95**, 044324 (2017)
- [3] S. Sels, T. Day Goodacre, B. A. Marsh, *Phys. Rev. C* **99**, 044306 (2019)
- [4] A. Barzakh, A. N. Andreyev, C. Raison, *Phys. Rev. Lett.* **127**, 192501 (2021)
- [5] S. Geldhof, M. Kortelainen, O. Beliuskina, *Phys. Rev. Lett.* **128**, 152501 (2022)
- [6] R. An, X.-X. Dong, L.-G. Cao, *Commun. Theo. Phys.* **75**, 035301 (2023)
- [7] H. Nakada, *Phys. Rev. C* **100**, 044310 (2019)
- [8] S. Bagchi, R. Kanungo, W. Horiuchi, *Phys. Lett. B* **790**, 251 (2019)
- [9] R. F. Garcia Ruiz and A. R. Vernon, *Eur. Phys. J. A* **56**, 136 (2020)
- [10] S. Kaur, R. Kanungo, W. Horiuchi, *Phys. Rev. Lett.* **129**, 142502 (2022)
- [11] U. C. Perera, A. V. Afanasjev and P. Ring, *Phys. Rev. C* **104**, 064313 (2021)
- [12] S. J. Novario, G. Hagen, G. R. Jansen, *Phys. Rev. C* **102**, 051303 (2020)
- [13] K. König, S. Fritzsche, G. Hagen, *Phys. Rev. Lett.* **131**, 102501 (2023)
- [14] A. E. Barzakh, A. N. Andreyev, T. E. Cocolios, *Phys. Rev. C* **95**, 014324 (2017)
- [15] M. Hammen, W. Nörtershäuser, D. L. Balabanski, *Phys. Rev. Lett.* **121**, 102501 (2018)
- [16] T. Day Goodacre, A. V. Afanasjev, A. E. Barzakh, *Phys. Rev. Lett.* **126**, 032502 (2021)
- [17] R. An, X. Jiang, L.-G. Cao, *Phys. Rev. C* **105**,

- 014325 (2022)
- [18] Y.-Y. Cao, J.-Y. Guo and B. Zhou, Nucl. Sci. Tech. **34**, 152 (2023)
- [19] L. Tang and Z.-H. Zhang, Nucl. Sci. Tech. **35**, 19 (2024)
- [20] M. Arnould M and S. Goriely, Prog. Part. Nucl. Phys. **112**, 103766 (2020)
- [21] N. Wang and T. Li, Phys. Rev. C **88**, 011301 (2013)
- [22] B. A. Brown, Phys. Rev. Lett. **119**, 122502 (2017)
- [23] B. A. Brown, K. Minamisono, J. Piekarewicz, et al., Phys. Rev. Res. **2**, 022035 (2020)
- [24] S. V. Pineda, K. König, D. M. Rossi, et al., Phys. Rev. Lett. **127**, 182503 (2021)
- [25] S. J. Novario, D. Lonardoni, S. Gandolfi, et al., Phys. Rev. Lett. **130**, 032501 (2023)
- [26] R. An, S. Sun, L.-G. Cao, et al., Nucl. Sci. Tech. **34**, 119 (2023)
- [27] Y.-N. Huang, Z.-Z. Li and Y.-F. Niu, Phys. Rev. C **107**, 034319 (2023)
- [28] M. Q. Ding, P. Su, D.-Q. Fang, et al., Chin. Phys. C **47**, 094101 (2023)
- [29] P. Bano, S. P. Pattnaik, M. Centelles, et al., Phys. Rev. C **108**, 015802 (2023)
- [30] K. König, J. C. Berengut, A. Borschevsky, et al., Phys. Rev. Lett. **132**, 162502 (2024)
- [31] S. Gautam, A. Venneti, S. Banik, et al., Nucl. Phys. A **1043**, 122832 (2024)
- [32] I. Angeli and K. Marinova, At. Data Nucl. Data Tables **99**, 69 (2013)
- [33] T. Li, Y. Luo and N. Wang, At. Data Nucl. Data Tables **140**, 101440 (2021)
- [34] A. Bohr and B. R. Mottelson, *Nuclear structure*. World Scientific Publishing Co. Pte. Ltd. (1969).
- [35] S. Q. Zhang, J. Meng, S.-G. Zhou, et al., Eur. Phys. J. A **13**, 285 (2002)
- [36] L. Yang, N. A. Alam, Z.-Z. Qin, et al., Robust correlation between binding energies and charge radii of mirror nuclei. ChinaXiv: 202412.00121 (2024). doi: 10.12074/202412.00121.
- [37] L.-S. Geng, H. Toki, S. Sugimoto, et al., Prog. Theor. Phys. **110**, 921 (2003)
- [38] R.-Y. Zheng, X.-X. Sun, G.-F. Shen, et al., Chin. Phys. C **48**, 014107 (2024)
- [39] S. Goriely, N. Chamel and J. M. Pearson, Phys. Rev. C **82**, 035804 (2010)
- [40] S. Goriely, S. Hilaire, M. Girod, et al., Phys. Rev. Lett. **102**, 242501 (2009)
- [41] I. Angeli and K. P. Marinova, J. Phys. G **42**, 055108 (2015)
- [42] P.-G. Reinhard and W. Nazarewicz, Phys. Rev. C **95**, 064328 (2017)
- [43] X.-R. Ma, S. Sun, R. An, et al., Chin. Phys. C **48**, 084104 (2024)
- [44] R. An, S. Sun, L.-G. Cao, et al., Nucl. Sci. Tech. **35**, 182 (2024)
- [45] G. A. Lalazissis and S. E. Massen, Phys. Rev. C **53**, 1599 (1996)
- [46] G. A. Miller, A. Beck, S. May-Tal Beck, et al., Phys. Lett. B **793**, 360 (2018)
- [47] L. A. Souza, Phys. Rev. C **101**, 065202 (2020)
- [48] U. C. Perera and A. V. Afanasjev, Phys. Rev. C **107**, 064321 (2023)
- [49] W. Cosyn and J. Ryckebusch, Phys. Lett. B **820**, 136526 (2021)
- [50] D. Zawischa, Phys.Lett. B **155**, 309 (1985)
- [51] D. Zawischa, U. Regge and R. Stapel, Phys.Lett. B **185**, 299 (1987)
- [52] R. An, L.-S. Geng and S.-S. Zhang, Phys. Rev. C **102**, 024307 (2020)
- [53] R. An, X. Jiang, L.-G. Cao, et al., Chin. Phys. C **46**, 064601 (2022)
- [54] R. An, S.-S. Zhang, L.-S. Geng and F.-S. Zhang, Chin. Phys. C **46**, 054101 (2022)
- [55] R. An, X. Jiang, N. Tang, et al., Phys. Rev. C **109**, 064302 (2024)
- [56] D. Yang, Y.-T. Rong, R. An, et al., Phys. Rev. C **110**, 004300 (2024)
- [57] M. Bender, P.-H. Heenen, and P.-G. Reinhard, Rev. Mod. Phys. **75**, 121 (2003)
- [58] X. Roca-Maza, L.-G. Cao, G. Colò, et al. Fully self-consistent study of charge-exchange resonances and the impact on the symmetry energy parameters. doi: 10.1103/PhysRevC.94.044313.
- [59] E.-B. Huo, K.-R. Li, X.-Y. Qu, et al., Nucl. Sci. Tech. **34**, 105 (2023)
- [60] E. Chabanat, P. Bonche, P. Haensel, et al., Nucl. Phys. A **627**, 710 (1997)
- [61] E. Chabanat, P. Bonche, P. Haensel, et al., Nucl. Phys. A **635**, 231 (1998)
- [62] J. Meng and P. Ring, Phys. Rev. Lett. **77**, 3963 (1996)
- [63] K. Wang and B.-N. Lu, Commun. Theo. Phys. **74**, 015303 (2022)
- [64] J. Meng, Nucl. Phys. A **635**, 3 (1998)
- [65] L.-G. Cao, H. Sagawa and G. Colò, Phys. Rev. C **86**, 054313 (2012)
- [66] S. Sun, S.-S. Zhang, Z.-H. Zhang and L.-G. Cao, Chin. Phys. C **45**, 094101 (2021)
- [67] M. Bender, K. Rutz, P.-G. Reinhard, et al., Eur. Phys. J. A **8**, 59 (2000)
- [68] K. Bennaceur and J. Dobaczewski, Comput. Phys. Commun. **168**, 96 (2005)
- [69] Y. K. Gambhir, P. Ring and A. Thimet, Ann. Phys. **198**, 132 (1990)
- [70] G. G. Dussel, S. Pittel, J. Dukelsky, et al., Phys. Rev. C **76**, 011302 (2007)
- [71] R. A. Broglia, F. Barranco, G. Potel, et al., Probable observation of the nuclear Cooper pair mean square radius in superfluid nuclei. arXiv: 2103.13536 (2023). arXiv: 2103.13536.
- [72] S. Malbrunot-Ettenauer, S. Kaufmann, S. Bacca, et al., Phys. Rev. Lett. **128**, 022502 (2022)
- [73] D. H. Youngblood, H. L. Clark and Y. W. Lui, Phys. Rev. Lett. **82**, 691 (1999)
- [74] M. Uchida, H. Sakaguchi, M. Itoh, et al., Phys. Rev. C **105**, 051301 (2004)
- [75] F. Sommer, K. König, D. M. Rossi, et al., Phys. Rev. Lett. **129**, 132501 (2022)
- [76] M. Kortelainen, Z. H. Sun, G. Hagen, et al., Phys. Rev. C **105**, L021303 (2022)
- [77] M. M. Sharma, G. Lalazissis, J. König, et al., Phys. Rev. Lett. **74**, 3744 (1995)
- [78] E. Caurier, K. Langanke, G. Martínez-Pinedo, et al., Phys.Lett. B **522**, 240 (2001)
- [79] R. F. Casten, D. S. Brenner and P. E. Haustein, Phys. Rev. Lett. **58**, 658 (1987)
- [80] I. Angeli, J. Phys. G **17**, 439 (1991)
- [81] Z.-Q. Sheng, G. W. Fan, J. F. Qian, et al., Eur. Phys. J. A

- [82] J. Xu, Z. Zhang and B.-A. Li, *Phys. Rev. C* **104**, 054324 (2021)
- [83] J. Yang and J. Pickarewicz, *Phys. Rev. C* **97**, 014314 (2018)
- [84] P.-G. Reinhard and W. Nazarewicz, *Phys. Rev. C* **105**, L021301 (2022)
- [85] B. S. Hu, *Phys. Lett. B* **857**, 138969 (2024)
- [86] M. Bhuyan, B. Maheshwari, H. A. Kassim, *et al.*, *J. Phys. G* **48**, 075105 (2021)
- [87] T. Naito, G. Colò, H.-Z. Liang, *et al.*, *Phys. Rev. C* **105**, L021304 (2022)
- [88] T. Naito, X. Roca-Maza, G. Colò, *et al.*, *Phys. Rev. C* **106**, L061306 (2022)
- [89] T. Naito, G. Colò, H.-Z. Liang, *et al.*, *Phys. Rev. C* **107**, 064302 (2023)
- [90] H. Yu, D.-Q. Fang, Y.-G. Ma, *Nucl. Sci. Tech.* **31**, 61 (2020)
- [91] Z.-Q. Feng, G.-M. Jin, *Phys. Lett. B* **683**, 140 (2010)
- [92] W.-J. Xie, J. Su, L. Zhu, *et al.*, *Phys. Lett. B* **718**, 1510 (2013)
- [93] M. Colonna, Y.-X. Zhang, Y.-J. Wang, *et al.*, *Phys. Rev. C* **104**, 024603 (2021)
- [94] G.-F. Wei, X. Huang, Q.-J. Zhi, *et al.*, *Nucl. Sci. Tech.* **33**, 163 (2022)
- [95] Z. Zhang and L.-W. Chen, *Phys. Rev. C* **108**, 024317 (2023)
- [96] S.-P. Wang, R. Wang, J.-T. Ye, *et al.*, *Phys. Rev. C* **109**, 054623 (2024)
- [97] M.-Q. Ding, D.-Q. Fang and Y.-G. Ma, *Nucl. Sci. Tech.* **35**, 211 (2024)
- [98] J. Xu, *Chin. Phys. Lett.* **38**, 042101 (2021)
- [99] W.-B. He, Q.-F. Li, Y.-G. Ma, Z.-M. Niu, J.-C. Pei, Y.-X. Zhang, *Sci. China Phys. Mech. Astron.* **66**, 282001 (2023)
- [100] D.-Q. Fang, *Nucl. Tech.* **46**, 155 (2023)
- [101] Z.-P. Gao and Q.-F. Li, *Nucl. Tech.* **46**, 95 (2023)
- [102] L. Liu, Y.-W. Lu, S. Sun and L.-G. Cao, *Chin. Phys. C* **49**, 024101 (2025)
- [103] J.-C. Zhang, B.-H. Sun, I. Tanihata, *et al.*, *Sci. Bull.* **69**, 1647 (2024)
- [104] J.-W. Zhao, B.-H. Sun, I. Tanihata, *et al.*, *Charge radii of ^{11–16}C, ^{13–17}N and ^{15–18}O determined from their charge-changing cross-sections and the mirror-difference charge radii*. doi: 10.1016/j.physletb.2024.139082.
- [105] J.-Y. Xu, Z.-Z. Li, B.-H. Sun, *et al.*, *Phys. Lett. B* **833**, 137333 (2022)